Chest CT Findings in Hospitalized Patients with SARS-CoV-2: Delta versus Omicron Variants

Soon Ho Yoon, MD, PhD* • Jong Hyuk Lee, MD, PhD* • Baek-Nam Kim, MD

From the Department of Radiology, Seoul National University Hospital, Seoul National University College of Medicine, Seoul, Korea (S.H.Y., J.H.L.); and Department of Internal Medicine, Inje University Sanggye Paik Hospital, Inje University College of Medicine, Seoul 01757, Korea (B.N.K.). Received March 20, 2022; revision requested May 2; revision received June 3; accepted June 6. **Address correspondence to** B.N.K. (email: *kimbn@paik.ac.kr*).

Background: CT manifestations of SARS-CoV-2 may differ among variants.

Purpose: To compare the chest CT findings of SARS-CoV-2 between the Delta and Omicron variants.

Materials and Methods: This retrospective study collected consecutive baseline chest CT images of hospitalized patients with SARS-CoV-2 from a secondary referral hospital when the Delta and Omicron variants were predominant. Two radiologists categorized CT images according to the RSNA classification system for COVID-19 and visually graded pneumonia extent. Pneumonia, pleural effusion, and intrapulmonary vessels were segmented and quantified on CT images using a priori–developed neural networks, followed by reader confirmation. Multivariable logistic and linear regression analyses were performed to examine the associations between the variants and CT category, distribution, severity, and peripheral vascularity.

Results: In total, 88 patients with the Delta variant (mean age, 67 years ± 15 [SD]; 46 men) and 88 patients with the Omicron variant (mean age, 62 years ± 19; 51 men) were included. Omicron was associated with less frequent, typical peripheral bilateral ground-glass opacity (32% [28 of 88] vs 57% [50 of 88], $P = .001$), more frequent peribronchovascular predilection (38% [25 of 66] vs 7% [five of 71], $P < .001$), lower visual pneumonia extent (5.4 ± 6.0 vs 7.7 ± 6.6, $P = .02$), similar pneumonia volume (5% ± 1 vs 7% ± 11, $P = .14$), and a higher proportion of vessels with a cross-sectional area smaller than 5 mm² relative to the total pulmonary blood volume (BV5%; 48% ± 11 vs 44% ± 8; $P = .004$). In adjusted analyses, Omicron was associated with a nontypical appearance (odds ratio, 0.34; $P = .006$), peribronchovascular predilection (odds ratio, 9.2; $P < .001$), and higher BV5% (β = 3.8; $P = .01$) but similar visual pneumonia extent ($P = .17$) and pneumonia volume ($P = .67$) relative to the Delta variant.

Conclusion: At chest CT, the Omicron SARS-COV-2 variant showed nontypical peribronchovascular pneumonia and less pulmonary vascular involvement than did the Delta variant in hospitalized patients with similar disease severity.

© RSNA, 2022

Online supplemental material is available for this article.

Since the COVID-19 pandemic began, SARS-CoV-2 has evolved through genetic mutations during viral replication (1,2). Several variants of SARS-CoV-2 have been reported worldwide throughout the pandemic, and some variants are classified as variants of concern due to increased transmissibility, disease severity, or evasiveness of treatments and vaccines (3). The Delta and Omicron variants are the two latest variants of concern (4,5).

The Delta variant was first identified in India in October 2020 and became the globally dominant strain in June 2021. This variant of concern has mutations that make it highly transmissible (>60% higher transmissibility than the previous variant), less responsive to antibodies and treatment (ie, reduced neutralization by antibodies generated against previous infection or vaccination), and more likely to cause adverse outcomes (eg, severe diesease, hospitalization, death) (6). Indeed, the Delta variant caused the second wave of India's pandemic and subsequent waves in other countries (7). The Omicron variant, which was first reported in November 2021 in South Africa, was designated as another variant of concern and has become the dominant strain after the Delta variant in most countries. Although the Omicron variant has up to 3.7 times higher transmissibility than the Delta variant, it is regarded as less virulent in terms of the rate of hospitalization, intensive care unit admissions, and mortality (8–10).

Chest CT plays a key role in the diagnosis, detection of complications, and potential prognostication in patients with COVID-19 (11,12). Previous studies have investigated differences between these two contiguously emerging dominant variants, with a focus on their spike proteins, diagnostic tests, clinical characteristics, transmissibility, and outcomes (9,10,13). However, it remains underexplored whether the CT findings of COVID-19 differ among variants. This study aimed to compare the chest CT findings of COVID-19 between the Delta and Omicron variants.

Abbreviations

BV5% = percentage of blood volume in intrapulmonary vessels with a cross-sectional area smaller than 5 mm^2 relative to the total pulmonary blood volume, GGO = ground-glass opacity

Summary

The Omicron SARS-CoV2 variant showed more frequent nontypical CT findings (peribronchovascular predilection, less pulmonary vascular involvement) than did the Delta variant in hospitalized patients with COVID-19 disease with comparable CT severity.

Key Results

- Only 32% of patients with the Omicron SARS-CoV-2 variant had typical CT appearances versus 57% of those with the Delta variant (P = .001).
- Peribronchovascular predilection was greater for the Omicron variant versus the Delta variant (38% vs 7%; P < .001).
- Pneumonia extent (P = .17) and volume (P = .67) did not differ between variants after adjustment for confounders of age, comorbidities, vaccination, and infection duration.

Materials and Methods

The institutional review board approved this retrospective study and waived informed consent (SGPAIK 2022–03–009).

Study Sample

This study was conducted at one of the secondary referral hospitals for the care of patients with mild to moderate COVID-19, which operated 30 beds for COVID-19. Inclusion criteria corresponded to patients with *(a)* polymerase chain reaction assay–proven SARS-CoV-2, *(b)* mild (no requirement for oxygen treatment) to moderate (a necessity for oxygen treatment with nasal prong or facial mask) COVID-19 severity at admission, and *(c)* risk factors for progression (Appendix E1 [online]). We excluded *(a)* patients who required care in the intensive care unit or ventilator support at admission, *(b)* pregnant patients, and *(c)* patients who chose not to undergo CT.

The hospital routinely performed baseline CT for hospitalized patients. We collected consecutive baseline CT images in November 2021 and February 2022 (Fig E1) when the Delta and Omicron variants were predominant in Korea, accounting for 99% and 97% of cases, respectively (14). All chest CT scans were obtained at full inspiration using CT scanners with at least 24 channels (Appendix E1 [online]).

We collected clinical and laboratory information, including infection duration at the time of CT (ie, days from symptom onset to CT) (15). The composite outcome was the occurrence of any of the following events: oxygen ventilation, intensive care unit admission, or death.

Visual CT Analysis

The randomly assigned baseline CT scans were independently evaluated by two board-certified thoracic radiologists (S.H.Y., J.H.L.; 17 and 10 years of clinical experience in thoracic imaging, respectively). They were aware that patients were infected with SARS-CoV-2 but were blinded to other clinical information, including the variant and dates of CT

examinations. Disagreement between the two radiologists was resolved by consensus.

CT images of COVID-19 pneumonia were classified into the following four categories according to the RSNA Expert Consensus Document, which was developed during the first wave of SARS-CoV2 infections (16): typical appearance, indeterminate appearance, atypical appearance, and negative for COVID-19 pneumonia (Appendix E1 [online]). For example, typical features of COVID-19 pneumonia include ground-glass opacities (GGOs) with or without consolidation in a peripheral, posterior, and diffuse or lower lung zone distribution and with a round appearance or a crazy paving pattern. Bronchial wall thickening, mucoid impactions, and nodules (tree-in-bud and centrilobular nodules), which are commonly seen in infections, are not typically observed.

Pneumonia extent was visually assessed using a scale of 0–5 for each of the five lung lobes (17): a score of 0 indicated no involvement; a score of 1, less than 5% involvement; a score of 2, 5%–25% involvement; a score of 3, 26%–49% involvement; a score of 4, 50%–75% involvement; and a score of 5, more than 75% involvement. The total CT score was the sum of the individual lobar scores and ranged from 0 (no involvement) to 25 (maximum involvement). The radiologists also assessed pneumonia density, predilected distribution (bronchovascular vs subpleural), lymphadenopathy, and pleural effusion (Appendix E1 [online]).

Quantitative CT Analysis

The CT images were processed using commercially available segmentation software (MEDIP PRO, version 2.0.0.0; MEDICALIP) using a priori–developed deep neural networks to segment the lung (18); COVID-19 pneumonia (19); pulmonary lobes and fissures and pulmonary vessels (20); and pleural effusion *(https://cris.nih.go.kr/cris/search/detailSearch.do/20687)*. The networks were updated with 3DnnU-Net (21), and the Dice similarity scores for those structures were 0.99 (lung), 0.84 (COVID-19), 0.98 (lobes), 0.91 (vessels), and 0.90 (effusion) in internal data sets.

A chest radiologist (S.H.Y.) reviewed and confirmed the segmentation masks. If any corrections were required, an imaging technician manually adjusted the masks under the instruction of the radiologist. The radiologist and technician were blinded to any clinical information other than the fact that the patients had COVID-19. The volume (in milliliters) of the segmented lung parenchymal and pneumonia masks was quantified to determine the proportion of COVID-19 pneumonia in the entire lung parenchyma and each lobe. The mean CT attenuation of COVID-19 was also calculated and converted into pneumonia weight (in grams) using an equation based on the CT attenuation and pneumonia volume (22). BV5% was calculated as the percentage of blood volume in intrapulmonary vessels with a cross-sectional area of less than 5 mm^2 relative to the total pulmonary blood volume (20). Lower BV5% reflected endothelial dysfunction and loss of microvasculature in COVID-19 (23,24). The volume of pleural effusion was quantified in milliliters, if present.

Statistical Analyses

Categorical variables were compared using the Fisher exact test and the χ^2 test, and continuous variables were compared using the t test or Mann–Whitney U test. Interreader agreements for visual assessment and total CT score were evaluated using the Cohen κ and intraclass correlation coefficient, respectively.

We examined the correlation between visual CT extent and pneumonia volume using the Pearson correlation coefficient. Multivariable logistic regression analysis was performed to examine the association of the variants with CT category and peribronchovascular predilection. Multivariable linear regression analyses were performed to examine the relationships between the variants and visual CT extent, pneumonia percentage, and weight, with the same adjustment. Multivariable Cox regression analyses were conducted to evaluate the association between the variants and the composite outcome. All multivariable analyses were conducted using an input function of confounders (Appendix E1 [online]). Infection duration was classified into five categories: 1, presymptomatic; 2, 0–2 days; 3, 3–5 days; 4, 6–11 days; and 5, more than 11 days (15).

Statistical analyses were conducted using SPSS software, version 25.0 (IBM), and a two-sided P value less than .05 indicated a significant difference.

Results

Clinical Characteristics of the Study Sample

Of 187 patients hospitalized with SARS-CoV-2, 11 were excluded because of pregnancy (n = 8) or reluctance to undergo CT (n = 3). The final study sampled consisted of 176 patients. Of these, 88 had the Delta variant (46 men, 42 women; mean age, 67 years ± 15 [SD]) and 88 had the Omicron variant (51 men, 37 women; mean age, 62 years ± 19). No patients reported previous infection with SARS-CoV-2. A flow diagram is given in Figure 1, and the clinical characteristics of this study sample are listed in Table 1.

Patients with the Omicron variant had higher levels of vaccination than did those with the Delta variant (unvaccinated, 28% [25 of 88] vs 32% [28 of 88]; partially vaccinated, 5% [four of 88] vs 6% [five of 88]; fully vaccinated: 23% [20 of 88] vs 62% [55 of 88]; booster vaccinated: 44% [39 of 88] vs 0% [0 of 88]; P < .001). The interval between symptom onset and CT was shorter in patients with the Omicron variant than in those with the Delta variant (mean, 3.9 days ± 3.2 vs 5.5 days ± 4.5; P = .01) in symptomatic patients. Other clinical characteristics, including age, sex, comorbidities, the proportion of asymptomatic patients at the time of CT, white blood cell count, lymphocyte count, lactate dehydrogenase level, proportion of patients requiring oxygen treatment, and proportion of unfavorable outcomes, showed no difference between the two variants (P > .05 for all) (Table 1).

Visual Assessment and Quantitative Assessment

The CT findings of the Omicron and Delta variants are described in Table 2. In terms of the RSNA COVID-19 imaging classification, the Omicron and Delta variants had different appearances (the proportions of typical appearance, indeterminate appearance, atypical appearance, and negative for pneumonia were 32% [28 of 88], 31% [27 of 88], 13% [11 of 88], and 25% [22 of 88], respectively, in patients with the Omicron variant and 57% [50 of 88], 20% [18 of 88], 3% [three of 88], and 19% [17 of 88], respectively, in patients with the Delta variant; P = .004). When appearance was dichotomized as typical or nontypical, patients with the Omicron variant had the typical CT appearance of COVID-19 pneumonia less frequently than did those with the Delta variant (32% [28 of 88] vs 57% [50 of 88], P = .001). The visual score of pneumonia extent was lower in patients with the Omicron variant (mean score, 5.4 ± 6.0) than in those with the Delta variant (mean score, 7.7 ± 6.6; P = .02). However, no evidence of differences was found between the two variants in the CT findings of visual assessment of pneumonia density (predominant GGO, predominant consolidation, and mixed pattern: 68% [45 of 66], 12% [eight of 66], and 20% [13 of 66], respectively, in the Omicron variant group vs 66% [47 of 71], 8% [six of 71], and 25% [18 of 71], respectively, in the Delta variant group; P = .61), the presence of lymphadenopathy (11% [10 of 88] vs 15% [13 of 88]; P = .66), or pleural effusion (18% [16 of 88] vs 22% [19 of 88]; P = .71).

In regard to interreader agreement for visual assessment of CT findings of the two variants, Cohen κ coefficients ranged from 0.51 to 0.81, with the highest value of 0.81 (95% CI: 0.74, 0.88) being for RSNA COVID-19 imaging classification and the lowest value of 0.51 (95% CI: 0.41, 0.61) being for pneumonia density. The intraclass correlation coefficient for pneumonia extent was 0.98 (95% CI: 0.98, 0.99).

In the quantitative CT analysis, patients with the Omicron variant had a higher BV5% than did those with the Delta variant (mean, 48% ± 11 vs 44% ± 8; P = .004). The mean CT attenuation (–404 HU ± 139 vs –402 HU ± 115; P = .92), quantitative analysis of pneumonia extent (5% ± 10 vs 7% ± 11, P = .14), pneumonia weight (95 g ± 174 vs 143 g ± 191, P = .09), and pleural effusion amount (275 mL ± 407 vs 149 mL ± 264, P = .47) showed no evidence of differences between the two variants (Figs 2–5). The Pearson correlation coefficient between visual pneumonia extent and pneumonia volume was 0.84.

Uni- and Multivariable Analyses for Effect of Omicron Variant Compared with Delta Variant

In the univariable analyses, patients with the Omicron variant had a lower frequency of a typical CT appearance (odds ratio, 0.36; P = .001), a more frequent peribronchovascular predilection (odds ratio, 8.0; P < .001), lower visual pneumonia extent (β = –2.3; P = .02), and greater BV5% (β = 4.4; P = .004) than patients with the Delta variant, whereas pneumonia volume (β = –2.3; P = .14), pneumonia weight (β = –47; P = .17), and 30-day composite outcomes were similar between the variants (hazard ratio, 1.8; P = .21) (Table 3).

After adjustment for confounders, multivariable analyses enabled us to confirm that patients with the Omicron variant less frequently had a typical CT appearance (odds ratio, 0.34; 95% CI: 0.16, 0.74; P = .006), more frequently had a peribronchovascular predilection (odds ratio, 9.2; 95% CI: 2.9, 28; P < .001), and had a greater BV5% (β = 3.8; 95% CI: 0.92, 6.8; P = .01) relative to those with the Delta variant. After adjustment,

there was no evidence of differences between the Omicron and Delta variants regarding visual pneumonia extent (β = −1.09, *P* = .17), pneumonia volume (β = −0.62, *P* = .67), pneumonia weight (β = −6.9, *P* = .82), and 30-day composite outcomes (hazard ratio, 3.1; *P* = .11; hazard ratio, 2.4; *P* = .29).

Significant confounders were identified in the multivariable analyses: The proportion of patients with a typical CT appearance was also greater with age (*P* = .006) and an infection duration of 6 days or longer (*P* < .001 to *P* = .004), whereas it was lower with full vaccination status (*P* = .006). The visual extent, pneumonia volume, and pneumonia weight also were greater with age (*P* < .001 to *P* = .009) and a longer infection duration (*P* < .001 for all) but were lower with full vaccination (*P* < .001 to *P* = .08). The BV5% was lower as pneumonia volume was greater (*P* = .001). CT severity was predictive of developing the 30-day composite outcome regardless of whether it was assessed visually or quantitatively (*P* = .002 for both).

Discussion

The CT manifestations of COVID-19 among different variants remain underexplored. We found that the Omicron variant was associated with a smaller proportion of patients with a typical CT appearance (32% [28 of 88] vs 57% [50 of 88], *P* = .001), a larger proportion of patients with peribronchovascular pneumonia (38% [25 of 66] vs 7% [five of 71], *P* < .001), a lower visual pneumonia extent (5.4 ± 6.0 vs 7.7 ± 6.6, *P* = .02), similar pneumonia volume (5% ± 10 vs 7% ± 11, *P* = .14), and a higher proportion of vessels with a cross-sectional area smaller than 5 mm² relative to the total pulmonary blood volume (BV5%) (48% ± 11 vs 44% ± 8, *P* = .004). After adjustment for confounders, including age, comorbidities, vaccination status, and infection duration, the Omicron variant was associated with a nontypical appearance (odds ratio, 0.34; *P* = .006), peribronchovascular predilection (odds ratio, 9.2; *P* < .001), and higher BV5% (β = 3.8, *P* = .01) but not with visual pneumonia extent (β = −1.09, *P* = .17) or pneumonia volume (β = −0.62, *P* = .67).

The frequency of a typical CT appearance has been reported to vary from 17% to 53% depending on the site and clinical indication (25–28), but our study sample with either variant underwent chest CT at the same site and for the same indications. Similar proportions of patients with either variant were unvaccinated or partially vaccinated, and these patients might be more likely to have a typical CT appearance (29). The odds of patients with the Omicron variant having a typical CT appearance and peribronchovascular predilection remained significant, even after adjustment for these confounders. The Omicron
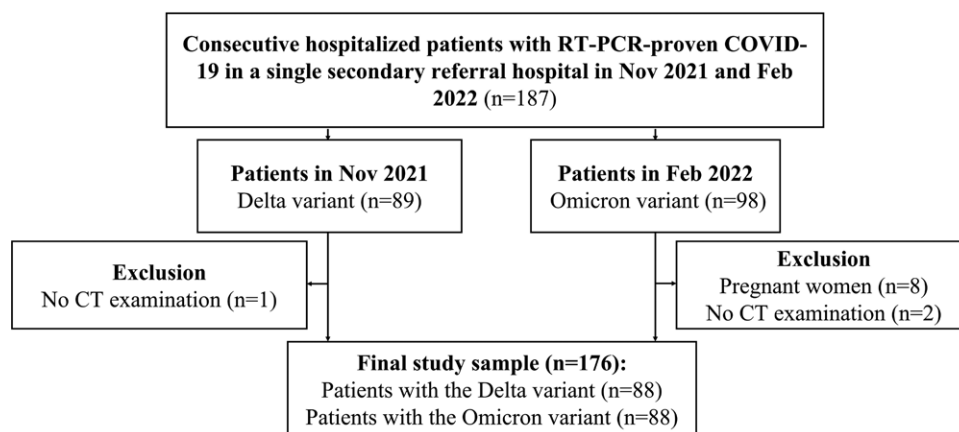
Figure 1: Flowchart of patient inclusion. RT-PCR = real-time reverse-transcription polymerase chain reaction.

Table 1: Clinical Characteristics of Patients with COVID-19 according to Variant

Clinical Characteristic	Delta Variant (*n* = 88)	Omicron Variant (*n* = 88)	*P* Value
Age (y)	67 ± 15	62 ± 19	.06
Male sex	46 (52)	51 (58)	.55
Presence of comorbidities*	73 (83)	67 (76)	.35
Vaccination status			<.001
Unvaccinated	28 (32)	25 (28)	…
Partially vaccinated	5 (6)	4 (5)	…
Fully vaccinated	55 (62)	20 (23)	…
Booster vaccinated	0 (0)	39 (44)	…
Infection duration†			
Presymptomatic	9 (10)	3 (3)	.009
0–2 days	22 (25)	31 (35)	…
3–5 days	24 (27)	38 (43)	…
6–11 days	26 (30)	13 (15)	…
>11 days	7 (8)	3 (3)	…
Complete blood count (cells/μL)	5920 ± 3063	6479 ± 3037	.23
Lymphocyte count (cells/μL)	1160 ± 656	1324 ± 627	.09
Lactate dehydrogenase (U/L)	555 ± 213	513 ± 214	.21
Oxygen treatment	27 (31)	24 (27)	.74
30-day composite outcome‡	7 (8)	12 (14)	.33

Note.—Unless otherwise noted, data are numbers of patients with percentages in parentheses or mean ± SD.

* Comorbidities included obesity, cardiovascular or cerebrovascular disease, immunocompromised status, diabetes mellitus, and chronic lung, liver, or renal disease.

† Infection duration was defined as days from symptom onset to CT examination.

‡ The composite outcome was defined as any of the following events: oxygen ventilation, intensive care unit admission, or death.

Table 2: Findings on Chest CT Scans of Patients with COVID-19 according to Variant

Finding	Delta Variant (n = 88)	Omicron Variant (n = 88)	P Value
RSNA COVID-19 imaging classification*			.004
Typical appearance	50 (57)	28 (32)	…
Indeterminate appearance	18 (20)	27 (31)	…
Atypical appearance	3 (3)	11 (13)	…
Negative for pneumonia	17 (19)	22 (25)	…
Score by visual assessment of pneumonia extent[†]	7.7 ± 6.6	5.4 ± 6.0	.02
Right upper lobe	1.3 ± 1.3	1.0 ± 1.3	.06
Right middle lobe	1.2 ± 1.3	0.9 ± 1.3	.08
Right lower lobe	1.8 ± 1.5	1.4 ± 1.5	.06
Left upper lobe	1.5 ± 1.4	1.0 ± 1.2	.005
Left lower lobe	1.9 ± 1.6	1.3 ± 1.5	.01
Visual assessment of pneumonia density[‡§]			.61
Predominant GGO	47 (66)	45 (68)	…
Predominant consolidation	6 (8)	8 (12)	…
Mixed pattern	18 (25)	13 (20)	…
Visual assessment of predominant distribution[§]			<.001
Peribronchovascular predilection	5 (7)	25 (38)	…
Subpleural predilection	43 (61)	22 (33)	…
Mixed pattern	23 (32)	19 (29)	…
Visual assessment for lymphadenopathy[§]	13 (15)	10 (11)	.66
Visual assessment for presence of pleural effusion	19 (22)	16 (18)	.71
Mean CT attenuation (HU)	−402 ± 115	−404 ± 139	.92
Pneumonia extent by quantitative CT analysis (%)	7 ± 11	5 ± 10	.14
Right upper lobe	5 ± 10	3 ± 8	.20
Right middle lobe	4 ± 9	3 ± 9	.38
Right lower lobe	11 ± 9	9 ± 18	.47
Left upper lobe	5 ± 10	3 ± 8	.16
Left lower lobe	11 ± 16	9 ± 18	.50
Pneumonia weight by quantitative CT analysis (g)	143 ± 191	95 ± 174	.09
Vessel <5 mm^2 (%)	44 ± 8	48 ± 11	.004
Pleural effusion amount (mL)	149 ± 264	275 ± 407	.47

Note.—Unless otherwise noted, data are numbers of patients, with percentages in parentheses, or mean ± SD. GGO = ground-glass opacity.

* The RSNA classification of COVID-19 on chest CT consists of the following: *(a)* typical appearance: peripheral bilateral GGOs or multifocal round GGOs with or without consolidation or intralobular lines, or reverse halo sign; *(b)* indeterminate appearance: presence of GGOs with or without consolidation but absence of typical features; *(c)* atypical appearance: absence of typical or indeterminate features with presence of lobar or segmental consolidation without GGOs, discrete centrilobular nodules, lung cavitation, or smooth interlobular septal thickening with pleural effusion; *(d)* negative for pneumonia: no CT features to suggest pneumonia.

[†] The total CT score was the sum of the individual lobar scores (each of the five lung lobes was visually scored on a scale of 0–5, with 0 indicating no involvement; 1, less than 5% involvement; 2, 5%–25% involvement; 3, 26%–49% involvement; 4, 50%–75% involvement; and 5, more than 75% involvement).

[‡] Pneumonia density was assessed in patients with pneumonia (71 with the Delta variant; 66 with the Omicron variant); predominant GGO: GGO to consolidation ratio ≥ 2:3; predominant consolidation: GGO to consolidation ratio <1:3; mixed pattern: 1:3 ≤ GGO to consolidation ratio < 2:3.

[§] Pneumonia density and predominant distribution were evaluated in cases with pneumonia (71 with Delta variant; 66 with Omicron variant).

[∥] Lymphadenopathy was considered present when mediastinal, interlobar, or supraclavicular lymph nodes were enlarged 1 cm or more in their short axis.

variant replicates better in the bronchi but worse in the lung parenchyma (13), and these characteristics may hinder infection with the Omicron variant from having a typical CT appearance when pneumonia is established in the lung parenchyma, while promoting peribronchovascular predilection.

BV5%, which reflects peripheral pulmonary volume and accounts for the majority of pulmonary blood volume (30), is lower in patients with SARS-CoV-2 than in healthy individuals and patients with acute respiratory distress syndrome (23,24). Furthermore, a lower BV5% was identified as a predictor of adverse clinical outcomes in COVID-19 (31). This characteristic reduction of BV5% in COVID-19 could result from SARS-CoV-2–induced vasoconstriction or microthrombi of small-caliber vessels (24). Indeed, SARS-CoV-2 inflames small vessels, provokes thrombi (32,33), and leads to frequent in situ pulmonary thrombosis, especially in patients with a severe
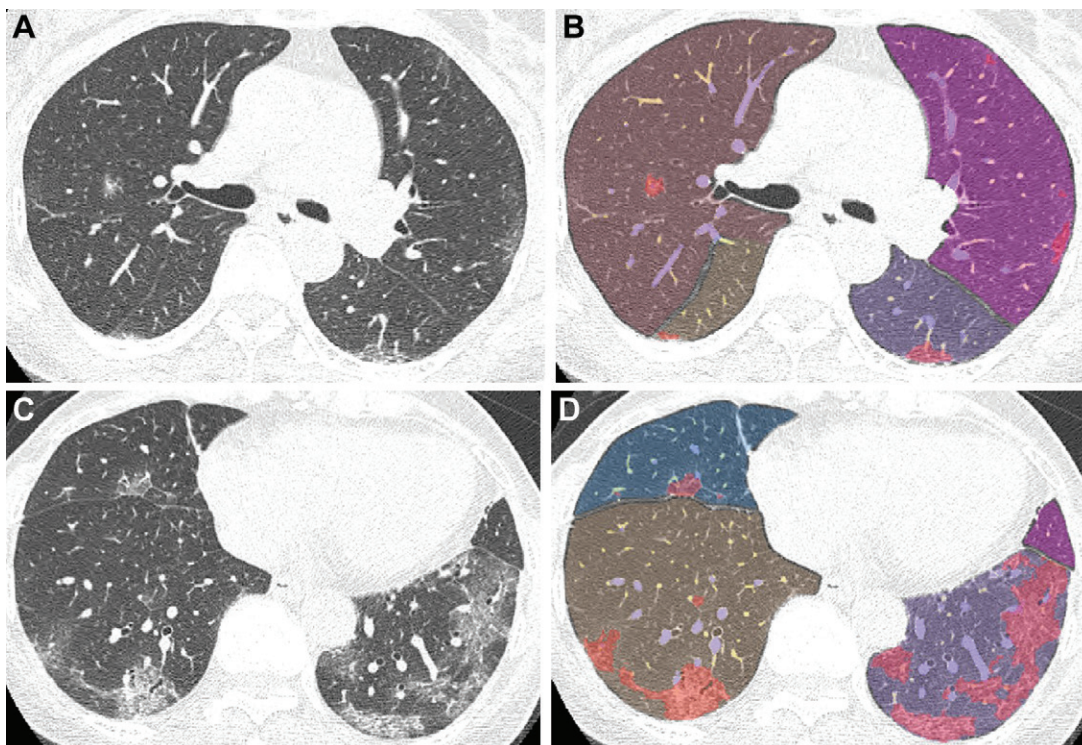
Figure 2: Chest CT images in a 66-year-old woman with the Delta variant of COVID-19 with a typical CT appearance. **(A, C)** Unenhanced axial CT images show peripheral bilateral ground-glass opacities with some intralobular lines predominantly involving both lower lobes. **(B, D)** Segmentation overlay images show the segmentation results of pneumonia (red), lobes (orange to violet), and pulmonary vessels, with a cross-sectional area less than 5 mm^2 (yellow) or 5 mm^2 or greater (blue). The visual CT score was 12 points, and the pneumonia volume was 9%.
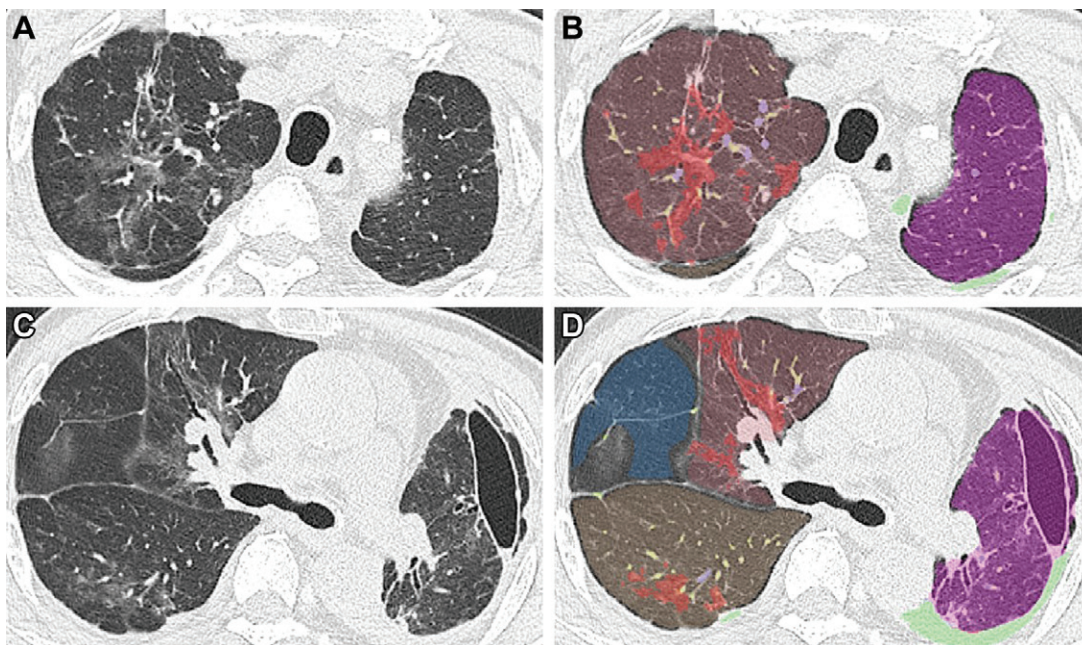
Figure 3: Chest CT images in a 77-year-old man with the Omicron variant of COVID-19 with indeterminate CT appearance. **(A, C)** Unenhanced axial CT images show unilateral peribronchovascular ground-glass opacities without intralobular lines or an apicobasal pre-dilection. **(B, D)** Segmentation overlay images show the segmentation results of pneumonia (red), lobes (orange to violet), effusion (light green), and pulmonary vessels with a cross-sectional area less than 5 mm^2 (yellow) and 5 mm^2 or greater (blue). The visual CT score was 13 points, and the pneumonia volume was 8%. A focal ground-glass opacity in the lateral portion of **D** was not included in the pneumonia mask because it was the minor fissure between the right upper and middle lobes.
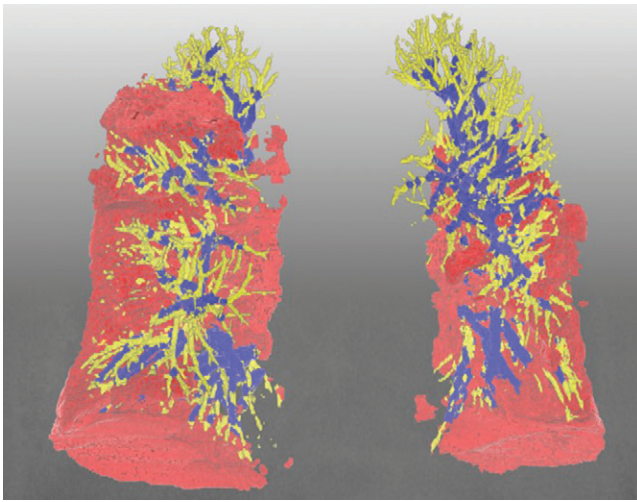
Figure 4: Representative three-dimensional chest CT image in an 88-year-old woman with the Delta variant of COVID-19 shows lower-lobe–predominant pneumonia (pneumonia volume, 14.7%) and a lower percentage of blood volume in intrapulmonary vessels, with a cross-sectional area less than 5 mm^2 relative to the total pulmonary blood volume (34.6%). Blue vessels have a cross-sectional area of 5 mm^2 or greater, and yellow vessels have a cross-sectional area less than 5 mm^2. Red indicates COVID-19 pneumonia.
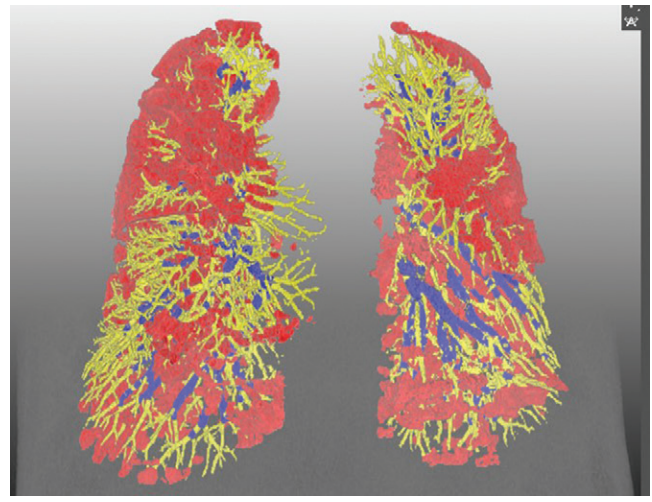
Figure 5: Representative three-dimensional chest CT image in a 52-year-old man with the Omicron variant of COVID-19 shows pneumonia evenly affecting lungs (pneumonia volume, 17.5%) and a preserved percentage of blood volume in intrapulmonary vessels, with a cross-sectional area less than 5 mm^2 relative to the total pulmonary blood volume (51.5%). Blue vessels have a cross-sectional area of 5 mm^2 or greater, and yellow vessels have a cross-sectional area less than 5 mm^2. Red indicates COVID-19 pneumonia.

Table 3: Effect of Omicron Variant Compared with Delta Variant on RSNA CT Classification System, CT Severity, Peripheral Vascularity, and Composite Outcome

Dependent Variable	Univariable Analysis		Multivariable Analysis	
	Odds Ratio, β Value, or Hazard Ratio	*P* Value	Odds Ratio, β Value, or Hazard Ratio	*P* Value
Logistic regression analysis				
Typical CT appearance for COVID-19*	0.36 (0.19, 0.66)	.001	0.34 (0.16, 0.74)	.006
Peribronchovascular predilection*	8.1 (2.9, 23)	<.001	9.2 (2.9, 29)	<.001
Linear regression analysis				
Visual extent	−2.3 (−4.2, −0.42)	.02	−1.09 (−2.6, 0.46)*	.17
Pneumonia volume (%)	−2.3 (−5.4, 0.79)	.14	−0.62 (−3.4, 2.2)*	.67
Pneumonia weight (g)	−47 (−113, 20)	.17	−6.9 (−67, 53)*	.82
BV5%	4.4 (1.4, 7.4)	.004	3.8 (0.92, 6.8)†	.01
Cox regression analysis				
30-day composite outcome adjusted with visual extent	1.83 (0.72, 4.7)	.21	3.08 (0.78, 12)‡	.11
30-day composite outcome adjusted with volume	…	…	2.37 (0.48, 11)§	.29

Note.—Odds ratios are reported for logistic regression analysis, β values are reported for linear regression analysis, and hazard ratios are reported for Cox regression analysis. Unless otherwise indicated, data are medians and data in parentheses are 95% CIs. The composite outcome comprised the occurrence of oxygen ventilation, intensive care unit admission, or mortality. BV5% = percentage of blood volume in intrapulmonary vessels with a cross-sectional area smaller than 5 mm^2 relative to total pulmonary blood volume.

* Adjusted for age, comorbidities, infection duration, and vaccination history. The proportion of a typical CT appearance also was greater with older age (*P* = .006) and longer infection duration (≥6 days, *P* < .001 to *P* = .004) but was lower with full vaccination (*P* = .006) in the multivariable analysis. In addition, visual extent, pneumonia volume, and pneumonia weight were greater with age (*P* < .001 to *P* = .009) and longer infection duration (all *P* < .001) but was lower with full vaccination (*P* < .001 to *P* = .084) in the multivariable analyses.

† Adjusted for age, comorbidities, infection duration, vaccination history, and pneumonia volume. The BV5% also was lower as pneumonia volume was greater (*P* = .001).

‡ Adjusted for age, comorbidities, infection duration, vaccination history, lymph node enlargement, pleural effusion, lymphocyte count, lactate dehydrogenase level, and visual pneumonia extent. A greater visual extent was the sole predictor of developing the 30-day composite outcome (*P* = .002) in the multivariable analysis.

§ Adjusted for age, comorbidities, infection duration, vaccination history, lymph node enlargement, pleural effusion, lymphocyte count, lactate dehydrogenase level, pneumonia volume, and BV5%. A larger pneumonia volume (*P* = .002) and a higher lactate dehydrogenase level (*P* = .035) were predictors of developing the 30-day composite outcome in the multivariable analysis.

case (34). Interestingly, early observations suggested that the Omicron variant might have a lower thrombosis rate than previous variants (35). This potentially provides support for the possibility that Omicron might involve fewer pulmonary vessels, in line with there being less involvement of the lower respiratory system.

Lower BV5% and CT vascular engorgement seem to result from the same vascular abnormalities of COVID-19 but manifest at different pulmonary vascular calibers. The cross-sectional vessel area of BV5% corresponds to a vascular diameter smaller than 1.26 mm, given the equation for a circle. These peripheral minute vessels had vasoconstriction or thrombosis but are too small to be visually assessed at CT. Meanwhile, vascular engorgement in patients with COVID-19 was typically observed in segmental or subsegmental vessels. The diameters were 3–4 mm or larger, corresponding to a cross-sectional vessel area of 28–50 mm^2 or larger. Vascular engorgement can reflect vascular dilatation or thrombosis proximal to SARS-CoV2–affected microvessels. Taken together, modern CT provided a multilevel analysis for revealing pulmonary vascular disease in patients with COVID-19 from impaired perfusion (vascular manifestation below a millimeter), lower peripheral BV5% (vascular manifestation around a millimeter), and proximally engorged vascular changes (vascular manifestation over a millimeter).

Our study had limitations. This study was retrospective and only included relatively few hospitalized patients. In addition, patient inclusion was conducted without calculating the sample size. Participants did not undergo testing to confirm the SARS-CoV-2 variant. Third, the clinical severity of hospitalized patients might not have been identical between variants, and the number of COVID-19 cases remained low in November 2021, when the Delta variant predominated, but soared in February 2022 with the Omicron variant. Fourth, the pulmonary vessels could not be segmented in consolidation areas on noncontrast CT images because the neural network and radiologist could not trace the vessels within consolidations. Fifth, we did not adjust for the multiplicity of tests in our analyses.

In conclusion, the Omicron variant showed more frequent nontypical peribronchovascular pneumonia and less pulmonary vascular involvement than did the Delta variant in hospitalized patients with comparable CT severity. The CT characteristics of Omicron may hamper radiologists from promptly recognizing COVID-19 on CT images when incidentally encountered, and this finding raises an alarm regarding the need to evaluate whether CT findings remain consistent or change when new variants appear.

Author contributions: Guarantors of integrity of entire study, J.H.L., B.N.K.; study concepts/study design or data acquisition or data analysis/interpretation, all authors; manuscript drafting or manuscript revision for important intellectual content, all authors; approval of final version of submitted manuscript, all authors; agrees to ensure any questions related to the work are appropriately resolved, all authors; literature research, all authors; clinical studies, S.H.Y., B.N.K.; statistical analysis, J.H.L., B.N.K.; and manuscript editing, all authors

References

1. Walensky RP, Walke HT, Fauci AS. SARS-CoV-2 variants of concern in the United States-challenges and opportunities. JAMA 2021;325(11):1037–1038.
2. Tao K, Tzou PL, Nouhin J, et al. The biological and clinical significance of emerging SARS-CoV-2 variants. Nat Rev Genet 2021;22(12):757–773.
3. Harvey WT, Carabelli AM, Jackson B, et al. SARS-CoV-2 variants, spike mutations and immune escape. Nat Rev Microbiol 2021;19(7):409–424.
4. Lopez Bernal J, Andrews N, Gower C, et al. Effectiveness of Covid-19 vaccines against the B.1.617.2 (Delta) Variant. N Engl J Med 2021;385(7):585–594.
5. Del Rio C, Malani PN, Omer SB. Confronting the delta variant of SARS-CoV-2, summer 2021. JAMA 2021;326(11):1001–1002.
6. Li B, Deng A, Li K, et al. Viral infection and transmission in a large, well-traced outbreak caused by the SARS-CoV-2 Delta variant. Nat Commun 2022;13(1):460.
7. Butt AA, Dargham SR, Chemaitelly H, et al. Severity of illness in persons infected with the SARS-CoV-2 delta variant vs beta variant in Qatar. JAMA Intern Med 2022;182(2):197–205.
8. Iuliano AD, Brunkard JM, Boehmer TK, et al. Trends in disease severity and health care utilization during the early omicron variant period compared with previous SARS-CoV-2 high transmission periods - United States, December 2020-January 2022. MMWR Morb Mortal Wkly Rep 2022;71(4):146–152.
9. Ulloa AC, Buchan SA, Daneman N, Brown KA. Estimates of SARS-CoV-2 omicron variant severity in Ontario, Canada. JAMA 2022;327(13):1286–1288.
10. Wolter N, Jassat W, Walaza S, et al. Early assessment of the clinical severity of the SARS-CoV-2 omicron variant in South Africa: a data linkage study. Lancet 2022;399(10323):437–446.
11. Rubin GD, Ryerson CJ, Haramati LB, et al. The role of chest imaging in patient management during the COVID-19 pandemic: a multinational consensus statement from the Fleischner Society. Radiology 2020;296(1):172–180.
12. Kwee TC, Kwee RM. Chest CT in COVID-19: what the radiologist needs to know. RadioGraphics 2020;40(7):1848–1865.
13. Hui KPY, Ho JCW, Cheung MC, et al. SARS-CoV-2 Omicron variant replication in human bronchus and lung ex vivo. Nature 2022;603(7902):715–720.
14. Korea COVID-19 update. Korea Disease Control and Prevention Agency. https://www.kdca.go.kr/board/board.es?mid=a20501010000&bid=20501010015. Accessed March 21, 2022.
15. Bernheim A, Mei X, Huang M, et al. Chest CT findings in coronavirus disease-19 (COVID-19): relationship to duration of infection. Radiology 2020;295(3):200463.
16. Simpson S, Kay FU, Abbara S, et al. Radiological Society of North America expert consensus document on reporting chest CT findings related to COVID-19: endorsed by the Society of Thoracic Radiology, the American College of Radiology, and RSNA. Radiol Cardiothorac Imaging 2020;2(2):e200152.
17. Wang Y, Dong C, Hu Y, et al. Temporal changes of CT findings in 90 patients with COVID-19 pneumonia: a longitudinal study. Radiology 2020;296(2):E55–E64.
18. Yoo SJ, Yoon SH, Lee JH, et al. Automated lung segmentation on chest computed tomography images with extensive lung parenchymal abnormalities using a deep neural network. Korean J Radiol 2021;22(3):476–488.
19. Yoo SJ, Qi X, Inui S, et al. Deep learning-based automatic CT quantification of coronavirus disease 2019 pneumonia: an international collaborative study. J Comput Assist Tomogr 2022;46(3):413–422.
20. Nam JG, Witanto JN, Park SJ, Yoo SJ, Goo JM, Yoon SH. Automatic pulmonary vessel segmentation on noncontrast chest CT: deep learning algorithm developed using spatiotemporally matched virtual noncontrast images and low-keV contrast-enhanced vessel maps. Eur Radiol 2021;31(12):9012–9021.
21. Isensee F, Jaeger PF, Kohl SAA, Petersen J, Maier-Hein KH. nnU-Net: a self-configuring method for deep learning-based biomedical image segmentation. Nat Methods 2021;18(2):203–211.
22. Choi H, Qi X, Yoon SH, et al. Extension of coronavirus disease 2019 on chest CT and implications for chest radiographic interpretation. Radiol Cardiothorac Imaging 2020;2(2):e200107 [Published correction appears in Radiol Cardiothorac Imaging 2020;2(2):e204001.].

23. Lins M, Vandevenne J, Thillai M, et al. Assessment of small pulmonary blood vessels in COVID-19 patients using HRCT. Acad Radiol 2020;27(10):1449–1455.

24. Thillai M, Patvardhan C, Swietlik EM, et al. Functional respiratory imaging identifies redistribution of pulmonary blood flow in patients with COVID-19. Thorax 2021;76(2):182–184.

25. de Jaegere TMH, Krdzalic J, Fasen BACM, Kwee RM; COVID-19 CT Investigators South-East Netherlands (CISEN) study group. Radiological Society of North America chest CT classification system for reporting COVID-19 pneumonia: interobserver variability and correlation with reverse-transcription polymerase chain reaction. Radiol Cardiothorac Imaging 2020;2(3):e200213.

26. Inui S, Kurokawa R, Nakai Y, et al. Comparison of Chest CT grading systems in coronavirus disease 2019 (COVID-19) pneumonia. Radiol Cardiothorac Imaging 2020;2(6):e200492.

27. Miranda Magalhães Santos JM, Paula Alves Fonseca A, Pinheiro Zarattini Anastacio E, Formagio Minenelli F, Furtado de Albuquerque Cavalcanti C, Borges da Silva Teles G. Initial results of the use of a standardized diagnostic criteria for chest computed tomography findings in coronavirus disease 2019. J Comput Assist Tomogr 2020;44(5):647–651.

28. Hammer MM. Real-world diagnostic performance of RSNA consensus reporting guidelines for findings related to COVID-19 on chest CT. AJR Am J Roentgenol 2022;218(1):75–76.

29. Lee JE, Hwang M, Kim YH, et al. Imaging and clinical features of COVID-19 breakthrough infections: a multicenter study. Radiology 2022;303(3):682–692.

30. Estépar RS, Kinney GL, Black-Shinn JL, et al. Computed tomographic measures of pulmonary vascular morphology in smokers and their clinical implications. Am J Respir Crit Care Med 2013;188(2):231–239.

31. Morris MF, Pershad Y, Kang P, et al. Altered pulmonary blood volume distribution as a biomarker for predicting outcomes in COVID-19 disease. Eur Respir J 2021;58(3):2004133.

32. Halawa S, Pullamsetti SS, Bangham CRM, et al. Potential long-term effects of SARS-CoV-2 infection on the pulmonary vasculature: a global perspective. Nat Rev Cardiol 2022;19(5):314–331.

33. Ackermann M, Verleden SE, Kuehnel M, et al. Pulmonary vascular endothelialitis, thrombosis, and angiogenesis in Covid-19. N Engl J Med 2020;383(2):120–128.

34. Suh YJ, Hong H, Ohana M, et al. Pulmonary embolism and deep vein thrombosis in COVID-19: a systematic review and meta-analysis. Radiology 2021;298(2):E70–E80.

35. Wilkinson E. Covid-19: We have good treatments for omicron, but questions remain, say doctors. BMJ 2022;376:o61.